Amorphization of embedded Cu nanocrystals by ion irradiation

B. Johannessen,[a] P. Kluth, and D. J. Llewellyn
Department of Electronic Materials Engineering, Research School of Physical Sciences and Engineering, Australian National University, Canberra, ACT 0200, Australia

G. J. Foran and D. J. Cookson
Australian Synchrotron Research Program, Australian Nuclear Science and Technology Organization, Menai, NSW 2234, Australia

M. C. Ridgway
Department of Electronic Materials Engineering, Research School of Physical Sciences and Engineering, Australian National University, Canberra, ACT 0200, Australia

(Received 10 December 2006; accepted 16 January 2007; published online 16 February 2007)

While bulk crystalline elemental metals cannot be amorphized by ion irradiation in the absence of chemical impurities, the authors demonstrate that finite-size effects enable the amorphization of embedded Cu nanocrystals. The authors form and compare the atomic-scale structure of the polycrystalline, nanocrystalline, and amorphous phases, present an explanation for the extreme sensitivity to irradiation exhibited by nanocrystals, and show that low-temperature annealing is sufficient to return amorphized material to the crystalline form. © *2007 American Institute of Physics*. [DOI: 10.1063/1.2644413]

Forming the amorphous phase of an elemental metal by rapid quenching from the molten state necessitates currently unattainable cooling rates of $>10^{10}$ °C/s.[1] While the addition of chemical impurities as glass formers impedes crystallization and lessens the cooling requirements, the final product is necessarily an alloy with properties that differ from the elemental metal. Alternative methods of forming the amorphous phase utilizing temperature extremes[2,3] have demonstrated some success for selected elemental metals. Ion implantation was once considered a promising alternative given the highly nonequilibrium nature of the ion stopping process in matter. As an ion slows, elastic collisions between the ion and lattice atoms can initiate a collision cascade of displaced atoms that exhibits a liquidlike character with a lifetime of $\sim 10^{-12}$ s.[4] Though the dissipation of residual kinetic energy to the lattice requires only a further $\sim 10^{-11}$ s,[5] elemental metals have only been amorphized by implanting chemical impurities.[6,7] Molecular-dynamics simulations confirmed that in the absence of glass formers, the recrystallization rate of a close-packed, metal-bonded lattice was simply too great to quench in the amorphous phase.[8] In the present letter, we show that embedded elemental Cu nanocrystals *can* be amorphized by ion implantation without the presence of chemical impurities. This fundamental finding represents a means of altering the structurally governed nanocrystal properties with the potential to enable advanced technological applications.

Elemental Cu nanocrystals with a volume-weighted average diameter of ~2.5 nm were formed in 2μm thick amorphous SiO_2, thermally grown on Si(100) substrates by ion implantation (~3.6 at. %) and thermal annealing (650 °C/1 h in forming gas).[9] X-ray diffraction (XRD), albeit with significantly broadened peaks due to finite-size effects, confirmed that the nanocrystals retained the bulklike face-centered-cubic (fcc) lattice structure. Nanocrystal samples and a bulk polycrystalline standard (220 nm thick) were then irradiated at −197 °C with 5 MeV Sn ions with a penetration depth significantly beyond that of the nanocrystals to negate impurity effects. The Sn ion dose (1×10^{14}/cm^2) was equivalent to ~0.16 displacements per Cu atom, with about half the beam energy dissipated in elastic collision processes.[10] Figure 1 shows cross-sectional transmission electron microscopy images of spherical nanocrystals in SiO_2 (a) before and (b) after irradiation. Lattice images of the (111) planes of fcc Cu superimposed on an amorphous SiO_2 matrix are discernible in the high-resolution inset in Fig. 1(a) with an estimated *d* spacing of 2.07±0.19 Å. Figure 1(b) shows that following irradiation nanometer-sized particles remained and the size distribution was qualitatively comparable to that of the unirradiated sample. However, XRD spectra were featureless (not shown) and the (111) lattice planes could no longer be imaged in the microscope, consistent with the lack of long-range order. (The XRD results are only indicative of amorphization and are not *conclusive* evidence due to the significant peak broadening associated with the finite nanocrystal size already prior to irradiation.) Hence, extended x-ray absorption fine structure (EXAFS) spectroscopy, capable of resolving structural details on an atomic level *without* the presence of long-range order, was utilized.

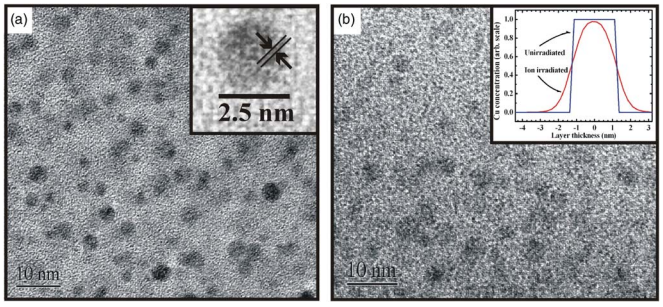

FIG. 1. (a) Transmission electron micrograph prior to irradiation [inset shows high-resolution image of an individual nanocrystal where the (111) planes of the fcc lattice are discernible] and (b) postirradiation image (inset shows the extent of ballistic mixing).

[a]Electronic mail: bej109@rsphysse.anu.edu.au

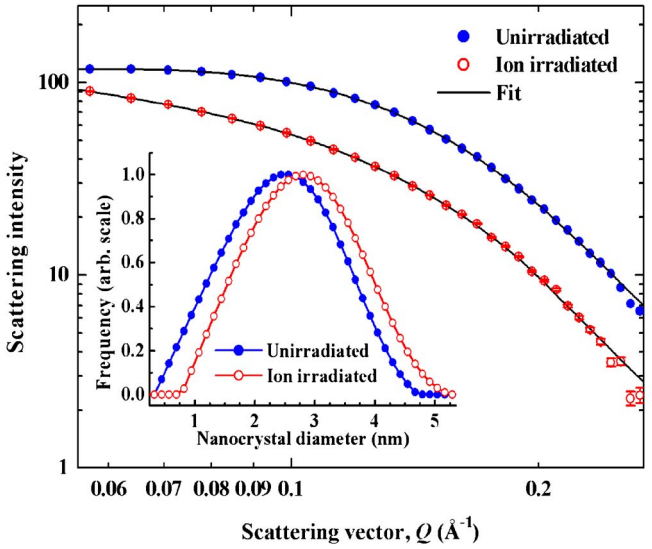

FIG. 2. (Color online) SAXS profiles for Cu nanocrystals before and after irradiation and (inset) their respective calculated size distributions.

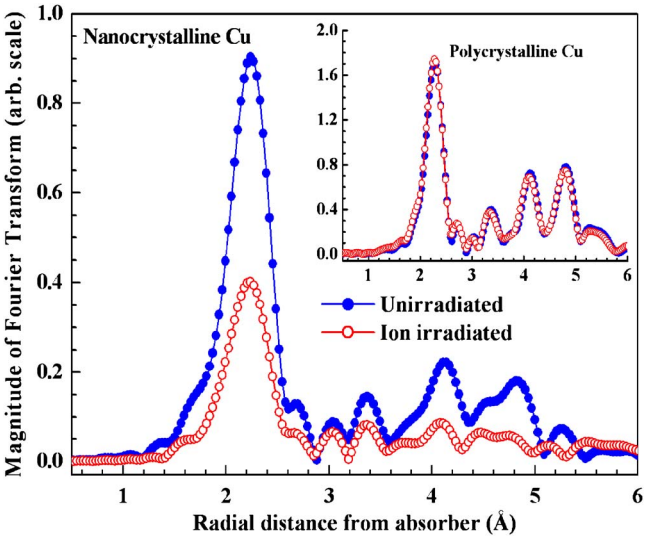

FIG. 3. (Color online) Fourier-transformed non-phase-corrected EXAFS spectra for Cu nanocrystals before and after irradiation and (inset) comparable spectra for a polycrystalline Cu standard.

Our electron microscopy observations were correlated with ion-dose-dependent binary-collision simulations[11] of Sn-induced atomic mixing for a Cu layer of 2.5 nm width in SiO_2 as shown in the Fig. 1(b) inset. Recoiling Cu, Si, and O atoms altered the Cu depth distribution from steplike to Gaussian-like yielding the less-well-defined nanocrystal/matrix interfaces evident in Fig. 1(b). Following irradiation, the fraction of Cu atoms in an oxidized state was quantified with x-ray absorption near-edge spectroscopy (XANES) from which only Cu metal and Cu_2O environments were apparent. (Irradiation with significantly higher ion doses yielded dissolution of nanocrystals as previously reported for Au.[12]) The net effect of irradiation, viewed simplistically, was a reduction in diameter of the elemental Cu core from ~2.5 to ~2.2 nm surrounded by a Cu_2O shell of ~0.6 nm thickness. Realistically, atomic mixing yielded a more diffuse nanocrystal/matrix interface. Changes in the nanocrystal size distribution were quantified with small-angle x-ray scattering[13] (SAXS) performed at 11.7 keV at the Advanced Photon Source in USA (beamline 15ID-D, ChemMatCARS) as shown in Fig. 2. The volume-weighted average diameter slightly increased after irradiation (~2.8 nm), consistent with our approximation above.

The atomic-scale structure surrounding Cu atoms was measured with EXAFS at the Photon Factory in Japan (beamline 20-B, The Australian National Beamline) performed in fluorescence mode at the Cu *K* edge at 12 K to minimize thermal disorder. Spectra were recorded to a photoelectron wave number (k) maximum of 18 $Å^{-1}$. The normalized EXAFS was k^3 weighted and Fourier transformed over a k range of 3.0–16.3 $Å^{-1}$, as shown in Fig. 3, and the first nearest-neighbor coordination shell was isolated by inverse transforming over a non-phase-corrected radial distance range of 1.74–2.74 Å, with extracted structural parameters listed in Table I. As anticipated, the Fig. 3 inset shows that the Fourier-transformed EXAFS spectrum of the polycrystalline standard was unchanged as a result of irradiation. To assess the potential influence of recoiled matrix atoms on the amorphization process, additional polycrystalline standards were implanted with Si and O ions (4 and 8 at. %, respectively) before irradiation. No changes in either the Fourier-transformed EXAFS or XRD were observed upon irradiation and thus, at these concentrations, Si and O impurities do not initiate or enable amorphization of the bulk.

Before irradiation, Table I shows that the nanocrystals exhibited structural differences, including a decreased bond length and increased Debye-Waller factor (structural disorder), relative to the polycrystalline standard. The former is the result of capillary pressure within the nanocrystal[14] while the latter is the result of bonding distortions at the nanocrystal/matrix interface.[15] The average number of Cu atoms surrounding each Cu atom (the nearest-neighbor coordination number) was reduced to 10.1+1.1 due to finite-size effects (undercoordinated surface atoms), as consistent with our theoretical calculation (10.2 atoms) determined from a knowledge of the fcc structure and the nanocrystal size distribution.[16]

Though neither the nanocrystal shape nor size was appreciably altered by irradiation, dramatic changes in the short-range order about a Cu atom were evident as shown in Fig. 3 and listed in Table I. These included a decreased Cu–Cu coordination number, an increased bond length and Debye-Waller factor, and a nonzero, positive value of the third cumulant (an asymmetric deviation from a Gaussian interatomic distance distribution skewed toward longer bond lengths). *All* such changes are consistent with theoretical predictions from a dense random packing (DRP) model for an elemental amorphous metal.[17] (We note that the latter can retain medium-range order,[18] evidence for which may be apparent in Fig. 3 beyond the first shell.) Though the structural parameters for the nanocrystal and amorphous phases are similar if one considers the associated fitting errors, the validity of such differences was confirmed using a ratio-method analysis.[19] The Cu–Cu interatomic distance distribution was reconstructed from the EXAFS measurements[20] shown in Fig. 4. Given the complementary electron microscopy and SAXS results presented above, we suggest the spectrum of irradiated nanocrystals represents the amorphous-phase structure. For comparison, the distance distribution for the DRP of hard spheres[17] is included. The experimental and theoretical distributions for the amorphous

TABLE I. EXAFS determinations of the structural parameters of unirradiated (unirr.) and ion irradiated (irr.) polycrystalline Cu (p-Cu) and Cu nanocrystals (Cu-nc). Note that the coordination numbers for the irradiated and recrystallized Cu nanocrystals have been corrected to account for the presence of Cu oxides as quantified by XANES analysis. Legend: recryst.=recrystallized, CN=coordination number, BL=bond length, DW=Debye-Waller factor, 3C=third cumulant, n/m=not measurable.

	CN (atoms)	BL (Å)	DW ($\times 10^{-3}$ Å^2)	3C ($\times 10^{-5}$ Å^3)
Unirr. p-Cu	12 (fixed)	2.539±0.001	2.3±0.1	n/m
Irr. p-Cu	12.3±0.6	2.541±0.005	2.4±0.6	n/m
Unirr. Cu-nc	10.1±1.1	2.520±0.006	4.9±0.7	0.6±8.0
Irr. Cu-nc	9.0±1.2	2.533±0.006	6.0±0.6	13.7±8.9
Recryst. Cu-nc	10.3±1.2	2.522±0.005	4.9±0.6	1.9±8.5

phase are similar and the marked asymmetry in both spectra is readily apparent.

After irradiation, the samples were thermally annealed (350 °C/1 h) under conditions sufficient to induce recrystallization yet insufficient for nanocrystal growth. The latter was verified with XANES measurements that showed the that fraction of Cu atoms in an oxidized state was unchanged upon annealing. As apparent from Table I, the structural parameters of the recrystallized and unirradiated samples were nearly identical. Equivalently, annealing reverses the nanoscale crystalline-to-amorphous phase transformation. We stress that the structural parameters of the amorphous phase listed in Table I are those for Cu–Cu bonding, distinguishable and separable from the Cu–O bonding resulting from recoiling nanocrystal and matrix atoms.

We suggest several factors enabled the ion-irradiation-induced crystalline-to-amorphous phase transformation for elemental Cu nanocrystals. Before irradiation, the nanocrystals were clearly perturbed relative to the polycrystalline standard. Though the fcc structure was retained, the inherent structural disorder (Debye-Waller factor) of the nanocrystals was twice that of the polycrystalline phase, potentially lowering the energy barrier for the amorphization process. During irradiation, disorder at the nanocrystal/matrix interface

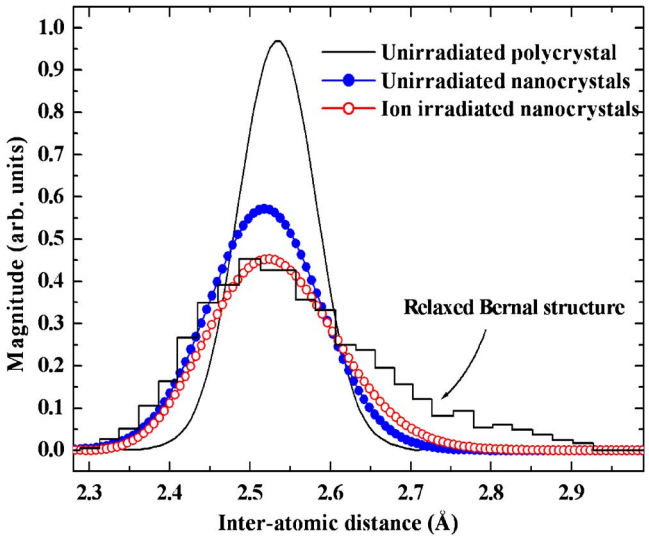

FIG. 4. (Color online) Radial distribution functions showing the first nearest-neighbor shell reconstructed from EXAFS data. A theoretical calculation for the DRP of hard spheres (relaxed Bernal structure) is shown.[17]

can serve as a preferential site for the nucleation of the amorphous phase and/or stabilize such a phase subsequent to formation. Given that half the Cu atoms reside at the interface, the influence thereof is necessarily great. This is in contrast to the irradiation of ~8 nm nanocrystals where <15% of the atoms reside at the interface and amorphization was not observed.[21] Finally, the recombination of vacancies and displaced atoms would necessarily be inhibited for Cu atoms recoiled beyond the nanocrystal bounds yielding an increased defect concentration for the nanocrystals relative to bulk polycrystalline material.

Our observation of metal nanocrystal amorphization follows our report that Ge nanocrystals could be amorphized with an irradiation dose nearly 100 times less than that required for its polycrystalline counterpart.[22] Evidently, finite-size effects render both semiconductor and metal nanocrystals significantly more sensitive to ion irradiation than the bulk phase.

The authors thank the Australian Synchrotron Research Program and the Australian Research Council for financial support. Use of the Advanced Photon Source was supported by the U.S. Department of Energy, Office of Science, Office of Basic Energy Sciences, under Contract No. DE-AC02-06CH11357.

[1] M. F. Ashby and D. R. H. Jones, *Engineering Materials 2—An Introduction to Microstructures, Processing and Design* (Pergamon, New York, 1986), 39, p. 89.
[2] T. Ichikawa, Phys. Status Solidi A **19**, 707 (1973).
[3] K. S. Suslick, S.-B. Choe, A. A. Cichowlas, and M. W. Grinstaff, Nature (London) **353**, 414 (1991).
[4] T. Diaz de la Rubia, R. S. Averback, R. Benedek, and W. E. King, Phys. Rev. Lett. **59**, 1930 (1987).
[5] K. Nordlund and R. S. Averback, Phys. Rev. B **56**, 2421 (1997).
[6] The one exception known to the authors is α-Ga that, in contrast to β-Ga, has been amorphized by implanting chemically inactive, noble-gas ions at a temperature of 10 K as demonstrated by M. Holz, P. Ziemann, and W. Buckel, Phys. Rev. Lett. **51**, 1584 (1983).
[7] P. M. Ossi, Mater. Sci. Eng. **90**, 55 (1987).
[8] K. Nordlund, M. Ghaly, R. S. Averback, M. Caturla, T. Diaz de la Rubia, and J. Tarus, Phys. Rev. B **57**, 7556 (1998).
[9] B. Johannessen, P. Kluth, C. J. Glover, G. de M. Azevedo, D. J. Llewellyn, G. J. Foran, and M. C. Ridgway, J. Appl. Phys. **98**, 024307 (2005).
[10] J. F. Ziegler, http://srim. org
[11] W. Moller and W. Eckstein, Nucl. Instrum. Methods Phys. Res. B **2**, 814 (1984).
[12] P. Kluth, B. Johannessen, G. J. Foran, D. J. Cookson, S. M. Kluth, and M. C. Ridgway, Phys. Rev. B **74**, 014202 (2006).
[13] C. S. Tsao and T. L. Lin, J. Appl. Crystallogr. **30**, 353 (1997).
[14] R. Meyer, L. J. Lewis, S. Prakash, and P. Entel, Phys. Rev. B **68**, 104303 (2003).
[15] P. Kluth, B. Johannessen, V. Giraud, A. Cheung, C. J. Glover, G. de M. Azevedo, M. C. Ridgway, and G. J. Foran, Appl. Phys. Lett. **85**, 3561 (2004).
[16] F. Boscherini, S. de Panfilis, and J. Weissmuller, Phys. Rev. B **57**, 3365 (1998).
[17] L. v. Heimendahl, J. Phys. F: Met. Phys. **5**, L141 (1975).
[18] D. B. Miracle, Nat. Mater. **3**, 697 (2004).
[19] G. Dalba, P. Fornasini, M. Grazioli, and F. Rocca, Phys. Rev. B **52**, 11034 (1995).
[20] G. Dalba and P. Fornasini, J. Synchrotron Radiat. **4**, 243 (1997).
[21] B. Johannessen, P. Kluth, C. J. Glover, S. M. Kluth, G. J. Foran, D. J. Cookson, D. J. Llewellyn, and M. C. Ridgway, Nucl. Instrum. Methods Phys. Res. B **250**, 210 (2006).
[22] M. C. Ridgway, G. de M. Azevedo, R. G. Elliman, C. J. Glover, D. J. Llewellyn, R. Miller, W. Wesch, G. J. Foran, J. Hansen, and A. Nylandsted-Larsen, Phys. Rev. B **71**, 094107 (2005).